metals

MDPI

Article

Multi-Objective Parameter Optimization for Cross-Sectional Deformation of Double-Ridged Rectangular Tube in Rotary Draw Bending by Using Response Surface Methodology and NSGA-II

Honglie Zhang, Yuli Liu * and Chunmei Liu

State Key Laboratory of Solidification Processing, School of Materials Science and Engineering, Northwestern Polytechnical University, Xi'an 710072, China; hliezhang@126.com (H.Z.); liuchunmei4321@sina.com (C.L.)

* Correspondence: lyl@nwpu.edu.cn; Tel.: +86-29-8846-0212

Academic Editor: Marek Muzyk

Received: 20 April 2017; Accepted: 31 May 2017; Published: 5 June 2017

Abstract: Cross-sectional deformation of double-ridged rectangular tube (DRRT) inevitably occurs due to the inhomogeneous deformation induced by external boundary conditions in rotary draw bending (RDB). Unreasonable factor combination would aggravate the cross-sectional deformation of DRRT. So, a powerful and efficient method combining Response Surface Methodology (RSM) and Non-Sorted Genetic Algorithm II (NSGA-II) was proposed to optimize the factors to control the cross-sectional deformation of DRRT in RDB. Firstly, an orthogonal experiment was used to screen out the important factors. It was obtained that three factors—clearance between DRRT and mandrel, clearance between DRRT and bending die, and boosting of pressure die—have an important influence on the cross-sectional deformation of DRRT. It can also be observed that the variation trend of flange sagging (FS) is always consistent with that of space deformation between ridges (SDR) with the changing of factors. RSM based on a Box-Behnken design was then used to establish response surface models. The proposed response surface models were used to analyze the relationship of the important parameters to the responses, such as space deformation between ridges, and width deformation of outer and inner ridge grooves (WDO and WDI). Finally, multi-objective parameter optimization for the cross-sectional deformation of DRRT in RDB was performed by using the established model and NSGA-II algorithm. The interaction of responses was revealed and the value range of each response in the space of Pareto optimal solutions was determined. It can be observed that there is always an evident conflict between SDR and WDO in the space of Pareto optimal solutions. By using this optimization method, the absolute values of SDR and WDI were significantly reduced—by 13.17% and 17.97%, respectively—compared with those before optimization, while WDO just increase only a little.

Keywords: multi-objective optimization; response surface methodology; genetic algorithm; cross-sectional deformation; double-ridged rectangular tube; rotary draw bending

1. Introduction

The bent double-ridged rectangular tube (DRRT) has been widely applied in communication devices used in aviation, aerospace, radar, and satellite for its advantages of lower cutoff frequency, wider operation bandwidth, lower characteristic impedance, and smaller loss [1]. In rotary draw bending (RDB), the cross-sectional deformation of DRRT inevitably occurs due to the inhomogeneous deformation induced by external boundary conditions [2], such as loading path and process parameter settings. In particular, unfavorable parameter combinations would aggravate the cross-sectional deformation of DRRT. Severe cross-sectional deformation brings about a serious loss of microwave

energy, which restricts the application of bent DRRT for microwave transmission. So, controlling the cross-sectional deformation of DRRT in RDB is critical for obtaining a sound bent DRRT. Due to the complicated profile, the cross-sectional deformation of DRRT needs to be characterized by several quality indexes. However, there are mutual conflicting effects of the several quality indexes; that is to say, a relative small value of one quality index is obtained by using certain a parameter combination while others are probably relative large. This makes it difficult to control the cross-sectional deformation of DRRT. Therefore, considering the interaction of several quality indexes, taking the quality indexes as objectives and conducting multi-objective parameter optimization is very important to improve the forming quality of DRRT in RDB.

In the past years, a lot of researchers have paid attention to the optimization of process parameters with multiple objectives in tube bending. To realize the control of spring back and section deformation, the sensitivity analysis method was used to obtain the processing parameters that have important effect on the defects in the bending process of rectangular tubes [3,4]. By developing a wrinkling energy prediction model, Yang et al. [5] obtained the appropriate forming parameters that guarantee no excessive thinning, severe flattening and wrinkling in RDB of aluminum alloy thin-walled tubes with large diameters. Based on an orthogonal experimental design and FEM analysis, Zhao et al. [6] achieved a reasonable clearance between tube and various dies for avoiding wrinkling and decreasing cross-sectional deformation in RDB of a rectangular tube. In order to keep wall thinning and flattening from exceeding certain values, the optimization for RDB of circular tubes was conducted by using the Response Surface Method (RSM), and the appropriate ranges of relative tube diameter and relative bending radius were determined [7]. It can be seen from the above reviews that parameter optimization with multiple objectives in tube bending is usually conducted based on a single method, such as sensitivity analysis, analytic method, orthogonal experimental design or response surface method. Furthermore, the interaction of the objectives was not taken into account in these methods. Nowadays, it is recognized that a single method cannot be used to sufficiently solve complex optimization problems with multiple objectives, and satisfactory results should be obtained by using hybrid methods [8]. Xiao et al. [9] performed the optimization of processing parameters for DRRT in RDB by combining an orthogonal test and grey relational analysis with a consideration of the interaction of multiple objectives. But this method can be only used to analyze the isolated points and cannot give intuitive graphics describing the relationship between the studied factors and responses. While, by using RSM combined with a genetic algorithm (NSGA-II), not only the interaction of multiple objectives are considered, but also the levels of each factor, can be continuously analyzed in the optimization process and an intuitive graphic can be given. Through the intuitive graphic, the interaction of factors contributing to the response can be better understood. Moreover, a global optimal solution for multi-objective optimization is able to be achieved accurately, instead of a local one [10]. Thus, RSM combined with genetic algorithm (NSGA-II) is increasingly used in multi-objective optimization [11,12].

The complexity of cross section for DRRT leads to the fact that its cross-sectional deformation needs to be evaluated by several quality indexes. Due to the mutually conflicting effects among the quality indexes, it is necessary to consider the interaction of them for controlling cross-sectional deformation of DRRT in the optimization process. Therefore, taking several quality indexes as objectives, a method combining RSM and NSGA-II is used to optimize the processing parameters for minimizing the cross-sectional deformation of DRRT in RDB. Firstly, the factors which have an important impact on the cross-sectional deformation of DRRT in RDB were selected by performing an analysis of variance (ANOVA) for the orthogonal experimental results. Then, RSM based on a Box-Behnken design was adopted to establish the response surface models relating the significant factors to each quality index of cross-sectional deformation of DRRT. By means of these models, the interaction of important factors on each quality index were evaluated. Finally, the multi-objective optimization for the cross-sectional deformation of DRRT in RDB was carried out based on the generated response surface models and NSGA-II algorithm.

2. The Multi-Objective Optimization Method for the Cross-Sectional Deformation of DRRT in RDB

2.1. The Rotary Draw Bending of DRRT

The property parameters of DRRT are listed in Table 1. The material is considered to be isotropic and the power exponent hardening model, $\sigma = K(\varepsilon_0 + \varepsilon)^n$, is used to express the material hardening behavior of the tube. For enhancing the computational efficiency and avoiding the phenomenon of shear locking, the double-ridged waveguide tube is discretized using 4-node doubly curved thin shell elements S4R; and the dies, including bending die, pressure die, wiper die, clamp die and mandrel-cores, are defined as discrete rigid bodies which are described by using 4-node 3D bilinear quadrilateral rigid elements C3D4. Meanwhile, the friction between tube and dies is modeled with the classical Coulomb friction model. Then, the FE (finite element) model of rotary draw bending of DRRT was established based on the platform of Abaqus/Explicit, as shown in Figure 1a. The RDB of DRRT is carried out under the constraint of multiple dies, including mandrel-core die, pressure die, wiper die, bending die and clamp die. The bending angle and bending radius are 90° and 40 mm, respectively. The clamp die is used to tightly clamp the tube, so there is no clearance or relative motion between clamp die and DRRT. Thus, the clearance and friction between DRRT and mandrel-core die (M clearance and M friction), pressure die (P clearance and P friction), wiper die (W clearance and W friction) and bending die (B clearance and B friction) are the factors that may have effects on the cross-sectional deformation of DRRT in RDB. In addition, the boosting of the pressure die also has an important effect on the cross-sectional deformation of DRRT. The boosting of the pressure die is denoted as Boosting and expressed in Equation (1),

$$\text{Boosting} = \frac{V_\text{p}}{w_0 R_0} \times 100\%, \tag{1}$$

where V_p is the boosting speed of the pressure die, w_0 is the angular velocity of the bending die and R_0 is the bending radius. Due to the complex profiles, the cross-sectional deformation of DRRT needs to be characterized by four quality indexes: flange sagging (FS), space deformation between ridges (SDR), width deformation of outer ridge groove (WDO), and width deformation of inner ridge groove(WDI), as shown in Equations (2)–(5),

$$\text{FS} = \frac{h' - h}{h} \times 100\%, \tag{2}$$

$$\text{SDR} = \frac{d' - d}{d} \times 100\%, \tag{3}$$

$$\text{WDO} = \frac{W' - W}{W} \times 100\%, \tag{4}$$

$$\text{WDI} = \frac{w' - w}{w} \times 100\%, \tag{5}$$

where h, d, W and w are the values of section height, space between ridges, outer ridge groove width and inner ridge groove width of DRRT before bending, as shown in Figure 1b. h', d', W' and w' are the corresponding values after bending. The values of the four quality indexes maybe positive or negative. A positive value represents that the value of the quality index after bending is bigger than that before bending deformation, while the negative value indicates that the value of the quality index after bending deformation is smaller than that before bending.

Table 1. Property parameters of double-ridged waveguide H96 tube.

Parameters	Elastic Modulus E (GPa)	Poisson Ratio υ	Yield Stress $\sigma_{0.2}$ (MPa)	Hardening Exponent n	Strength Coefficient k (MPa)
Value	92.81	0.324	70	0.56	588.17

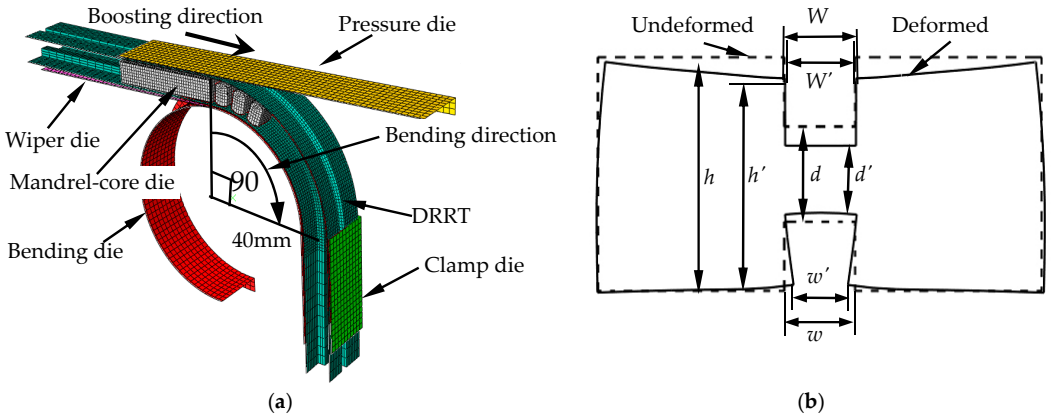

Figure 1. The RDB of DRRT and the description of cross-sectional deformation of DRRT: (**a**) The sketch of RDB of DRRT; (**b**) the description of cross-sectional deformation of DRRT.

In order to verify the reliability of the FE model, a numerical simulation and experiment of RDB of DRRT were conducted. The experiment was conducted on a W27YPC-63 PLC controlled hydraulic tube bender (Shanghai Guoqing Machinery Co., Ltd, Shanghai, China). The processing parameters in the simulation and experiment are listed in Table 2. Based on these conditions, the FE model of RDB of DRRT was verified by the experiment in Reference [13] and it was concluded that the FE model is reliable.

Table 2. Forming parameters used in experiment and simulation.

Parameters	Experiment	Simulation
Bending velocity (rad/s)	0.5	0.5
Bending radius (mm)	40	40
Bending angle (°)	90	90
Boosting velocity (mm/s)	22.6	22.6
Friction between tube and core	Hydraulic oil	0.03
Friction between tube and clamp die	Dry friction	Rough
Friction between tube and other dies	Dry friction	0.19
Clearances between tube and core (mm)	0.175	0.175
Clearances between tube and other dies (mm)	0	0

2.2. The Detailed Procedure of Multi-Objective Optimization

Figure 2 shows the detailed procedure of multi-objective optimization for cross-sectional deformation of DRRT in RDB. There are nine factors—M clearance, P clearance, W clearance, B clearance, M friction, P friction, W friction, B friction and Boosting—than influence the cross-sectional deformation of DRRT in RDB. At first, the FE simulations were conducted based on the orthogonal experimental design by using a reliable FE model of RDB of DRRT developed in a previous study [13]. By performing ANOVA for the simulation results, the factors that have important effects on the cross-sectional deformation of DRRT were selected from the nine factors.

Then, a Box-Behnken Design (BBD) was used to conduct the design of an experiment for important factors. Compared to Central Composite Design, BBD just requires that each factor has three levels and needs the least number of experiments. The FE simulations of RDB of DRRT were conducted according to BBD, and a response surface model relating important factors to the response was established. Generally, a quadratic response surface model is adequate, and its polynomial equation is expressed in Equation (6),

$$Y = \beta_0 + \sum_{i=1}^{k} \beta_i x_i + \sum_{i=1}^{k} \beta_{ii} x_i^2 + \sum_{i=1}^{k} \sum_{j=i+1}^{k} \beta_{ij} x_i x_j, \quad (6)$$

where Y is the response. β_0, β_i, β_{ii} and β_{ij} are the coefficients of intercept, linear, quadratic and interactive terms, respectively. x_i and x_j are important factors. By means of the model, the interaction of significant factors on the response can be evaluated.

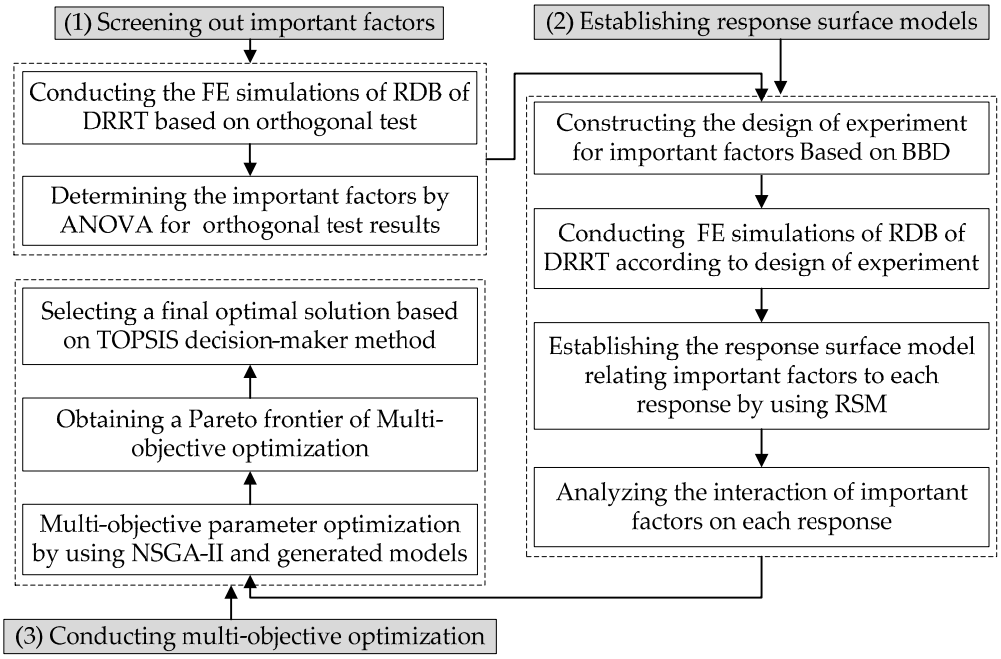

Figure 2. The flow chart of multi-objective optimization for the cross-sectional deformation of DRRT in RDB.

Finally, taking the quality indexes of cross-sectional deformation as objectives, the multi-objective parameter optimization for the cross-sectional deformation of DRRT in RDB was performed based on the generated response surface models and NSGA-II. For a multi-objective optimization problem, it is impossible to find a unique solution which can optimize all the objectives simultaneously, because the objectives are usually mutually conflicting. By using NSGA-II, a set of non-dominated solutions termed as Pareto optimal solutions can be obtained [14]. The set of Pareto optimal solutions is defined as the Pareto frontier of multi-objective optimization. Thus, a Pareto frontier of multi-objective parameter optimization for the cross-sectional deformation of DRRT in RDB was obtained by using NSGA-II. Moreover, in order to meet the requirement of practical operation, a final optimal solution was selected from the Pareto frontier based on the TOPSIS (Technique for Order Preference by Similarity to an Ideal Solution) decision-maker method.

3. Results and Discussion

3.1. The Determination of Significant Factors and Responses

3.1.1. Selection of Significant Factors Based on Orthogonal Experiment

Before conducting the optimization process, the orthogonal experiment was initially adopted to select the important factors from the nine factors shown in Table 3, and each factor was assigned three levels (−1, 0, +1).

Based on the orthogonal experiment design, 27 FE simulations with different factor combinations were conducted. An analysis of variance (ANOVA) for the simulation results was performed and the *F*-values (Fischer variation ratio) presenting the importance of factors were obtained, as shown in Table 4. In order to more clearly determine the importance of one factor, the ANOVA for the simulation results were also presented in bar chart form, as shown in Figure 3. It can be seen that the three factors

M clearance, B clearance and Boosting have important effects on cross-sectional deformation of DRRT in RDB.

Table 3. Levels of factors in the orthogonal experiment.

Factors	Low (−1)	Middle (0)	High (+1)
M clearance (mm)	0.1	0.2	0.3
P clearance (mm)	0.1	0.2	0.3
W clearance (mm)	0.1	0.2	0.3
B clearance (mm)	0.1	0.2	0.3
M friction	0.02	0.08	0.14
P friction	0.14	0.22	0.30
W friction	0.06	0.14	0.22
B friction	0.06	0.14	0.22
Boosting (%)	80	90	100

Table 4. The ANOVA for the orthogonal experiment.

Factors	*F*-Value				Critical Value	Remarks			
	FS	SDR	WDO	WDI		FS	SDR	WDO	WDI
M clearance	66.81	65.23	5.71	9.82		***	***	**	***
P clearance	0.11	0.27	0.46	1.68	$F_{0.01}(2, 8) = 8.65$				
W clearance	0.09	0.06	0.34	1.87					
B clearance	36.64	23.29	3.08	63.60		***	***		***
M friction	0.41	0.99	1.04	1.21	$F_{0.05}(2, 8) = 4.46$				
P friction	0.27	0.23	0.43	0.24					
W friction	0.59	0.17	1.99	0.66					
B friction	1.14	2.29	3.04	0.84	$F_{0.1}(2, 8) = 3.11$				
Boosting	7.78	8.82	0.96	3.59		**	***		*

*** indicates that the factor has a highly important impact on response and $F > F_{0.01}$; ** indicates that the factor has an important impact on response and $F_{0.01} > F > F_{0.05}$; * indicates that the factor has an impact on response and $F_{0.05} > F > F_{0.1}$. "Blank" indicates that the factor has little impact on response.

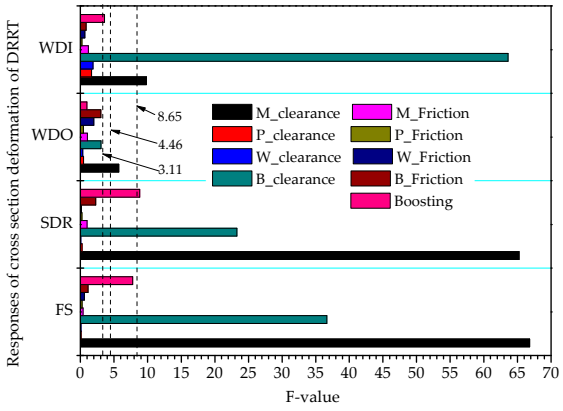

Figure 3. The importance of one factor to one response.

3.1.2. The Determination of Responses in RSM

In the process of multi-objective parameter optimization for the cross-sectional deformation of DRRT in RDB, the four quality indexes of cross-sectional deformation—FS, SDR, WDO and WDI—are probably used as responses in the establishment of response surface models. However, as can be seen from Figure 4a, which shows the distribution of four quality indexes obtained from FE simulations based on the orthogonal experiment, the variation of FS is always consistent with that of SDR with the changing of factors. That is to say that the influence laws of factors on FS and SDR are completely the same. So, taking only one of them as the study objective is enough. Whereas, the variation trend

of WDO is quite different from that of WDI, as shown in Figure 4b. Thus, in order to simplify the optimization process, SDR, WDO and WDI were selected as the responses in RSM.

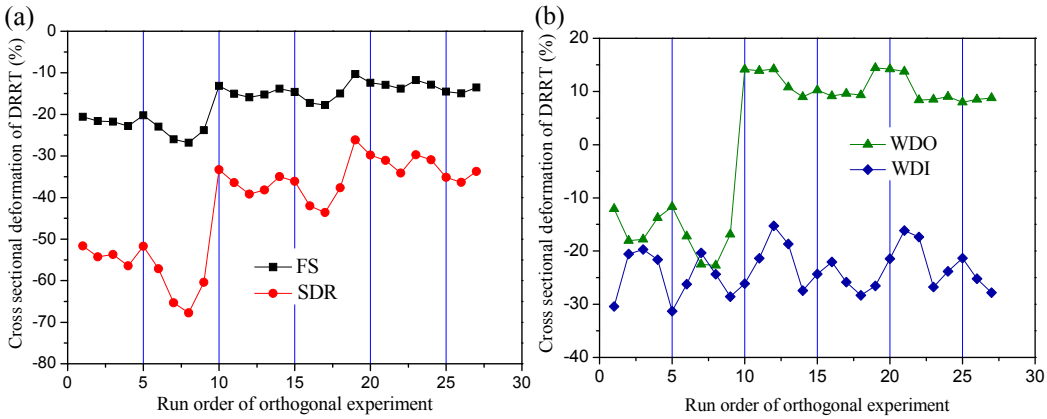

Figure 4. The cross-sectional deformation of DRRT obtained from FE simulations based on the orthogonal experiment: (**a**) FS and SDR; (**b**) WDO and WDI.

3.2. Design of the Experiment according to BBD

After the determination of important factors, a BBD in which each important factor has three levels (−1, 0, +1) was used to perform the design of the experiment for establishing a response surface model, while the unimportant factors in Table 3 were kept constant at the middle level. So, a total of 15 FE simulations needed to be performed according to BBD in this study, as shown in Table 3. Design Expert 8.0.6 was used to conduct the design of experiment and establish the response surface models. The simulation results of SDR, WDO and WDI are also recorded in Table 5.

Table 5. Three factorial Box-Behnken design and the results.

Factors	**Low (−1)**		**Middle (0)**		**High (+1)**	
M clearance (mm)	0.1		0.2		0.3	
B clearance (mm)	0.1		0.2		0.3	
Boosting (%)	80		90		100	
No	M clearance	B clearance	Boosting	SDR (%)	WDO (%)	WDI (%)
1	0.2	0.1	80	−25.93	7.95	−22.15
2	0.1	0.2	80	−25.99	14.18	−17.47
3	0.2	0.1	100	−21.98	7.421	−22.58
4	0.3	0.1	90	−27.20	5.70	−22.46
5	0.2	0.2	90	−25.17	7.55	−18.23
6	0.2	0.3	100	−21.34	7.32	−19.54
7	0.3	0.3	90	−26.82	5.69	−19.21
8	0.3	0.2	80	−27.13	5.42	−18.94
9	0.2	0.2	90	−25.25	7.45	−18.13
10	0.3	0.2	100	−24.66	6.68	−19.45
11	0.2	0.2	90	−25.05	7.65	−18.33
12	0.1	0.2	100	−19.31	13.68	−18.445
13	0.2	0.3	80	−26.97	7.90	−17.79
14	0.1	0.3	90	−23.83	13.99	−17.56
15	0.1	0.1	90	−24.07	14.02	−21.98

3.3. Establishment of Response Surface Models and Analysis of Factor Interaction

3.3.1. Establishment of Response Surface Models and Their Evaluation

(1) Establishing the response surface models by analysis of variance

An analysis of variance (ANOVA) on the simulation results in Table 5 was performed to estimate the coefficients of the polynomial equation in Equation (6). The ANOVA results for the responses SDR,

WDO and WDI are shown in Tables 6–8, respectively. Statistical significance was checked by *F*-value and *p*-value (significant probability value). Terms whose *p*-value is less than 0.05 have a significant effect on the response [11]. Based on the ANOVA results, the equations of the response surface models, which relate the significant factors (M clearance, B clearance and Boosting, which are marked as *A*, *B* and *C*, respectively) to responses, were obtained, as shown in Equations (7)–(9),

$$\text{SDR} = 38.18 + 89.86 \times A - 37.51 \times B - 1.72 \times C - 1.05 \times A \times C + 0.42 \times B \times C - 26.96 \times A^2 + 0.01 \times C^2, \quad (7)$$

$$\text{WDO} = 33.29 - 172.72 \times A - 0.09 \times C + 0.44 \times A \times C + 231.57 \times A^2, \quad (8)$$

$$\text{WDI} = -53.98 + 0.11 \times A + 134.26 \times B + 0.51 \times C - 29.34 \times A \times B - 0.33 \times B \times C - 199.95 \times B^2, \quad (9)$$

Table 6. ANOVA for SDR.

Source	Sum of Squares	df	Mean Square	*F*-Value	*p*-Value (Prob > *F*)	Significance
Model	74.32	7	10.62	367.27	<0.0001	significant
M clearance (*A*)	19.88	1	19.88	687.6	<0.0001	-
B clearance (*B*)	5.84×10^{-3}	1	5.84×10^{-3}	0.2	0.6666	-
Boosting (*C*)	43.84	1	43.84	1516.59	<0.0001	-
$A \times C$	4.44	1	4.44	154	<0.0001	-
$B \times C$	0.71	1	0.71	24.39	0.0017	-
A^2	0.27	1	0.27	9.32	0.0185	-
C^2	4.98	1	4.98	172.42	<0.0001	-
Residual	0.2	7	2.90×10^{-2}	-	-	-
Lack of Fit	0.18	5	0.036	3.62	0.2305	not significant
Pure Error	0.02	2	0.01	-	-	-
Cor Total	74.52	14	-	-	-	-
R^2	0.9973		-	-	-	-

Table 7. ANOVA for WDO.

Source	Sum of Squares	df	Mean Square	*F*-Value	*p*-Value (Prob > *F*)	Significance
Model	151.88	4	37.97	619.71	<0.0001	significant
M clearance (*A*)	131.06	1	131.06	2139.18	<0.0001	-
Boosting (*C*)	1.60×10^{-2}	1	1.60×10^{-2}	0.26	0.621	-
$A \times C$	0.77	1	0.77	12.65	0.0052	-
A^2	20	1	20	327	<0.0001	-
Residual	0.61	10	0.061	-	-	-
Lack of Fit	0.59	8	7.40×10^{-2}	7.41	0.1243	not significant
Pure Error	0.02	2	0.01	-	-	-
Cor Total	152	14	-	-	-	-
R^2	0.9960	-	-	-	-	-

Table 8. ANOVA for WDI.

Source	Sum of Squares	df	Mean Square	*F*-Value	*p*-Value (Prob > F)	Significance
Model	48.41	7	6.92	281.63	<0.0001	significant
M clearance (*A*)	2.65	1	2.65	107.93	<0.0001	-
B clearance (*B*)	28.4	1	28.4	1156.63	<0.0001	-
Boosting (C)	1.67	1	1.67	67.94	<0.0001	-
$A \times B$	0.34	1	0.34	14.02	0.0072	-
$B \times C$	0.43	1	0.43	17.59	0.0041	-
B^2	14.85	1	14.85	604.75	<0.0001	-
C^2	0.28	1	0.28	11.27	0.0121	-
Residual	0.17	7	0.025	-	-	-
Lack of Fit	0.15	5	0.03	3.04	0.266	not significant
Pure Error	0.02	2	0.01	-	-	-
Cor Total	48.58	14	-	-	-	-
R^2	0.9965	-	-	-	-	-

(2) Evaluation of the response surface models

The quality of fit of the polynomial model was evaluated by Lack of Fit and determination coefficient R^2. Lack of Fit is a statistical test that gives information on the adequacy of the model fit under consideration. If the model does not fit the experimental data of design points well, this will be significant. As shown in Tables 6–8, for the models of SDR, WDO and WDI, the Lack of Fit is not significant, indicating a good fit to the models. The determination coefficients R^2 for SDR, WDO and WDI are all close to 1, which implies that the models are adequate for representing the relationship between the factors and each response. In order to further estimate the adequacy of the models, the predicted values of the design points in Table 5 obtained by the generated models were compared with the simulation values, as shown in Figure 5. It can be seen that the points of predicted values versus simulation values all fall near the 45° lines, with some deviation in an acceptable range of error. From the discussion above, it can be concluded that the established response surface models are reliable, and capable of expressing the relationship between important factors and response accurately.

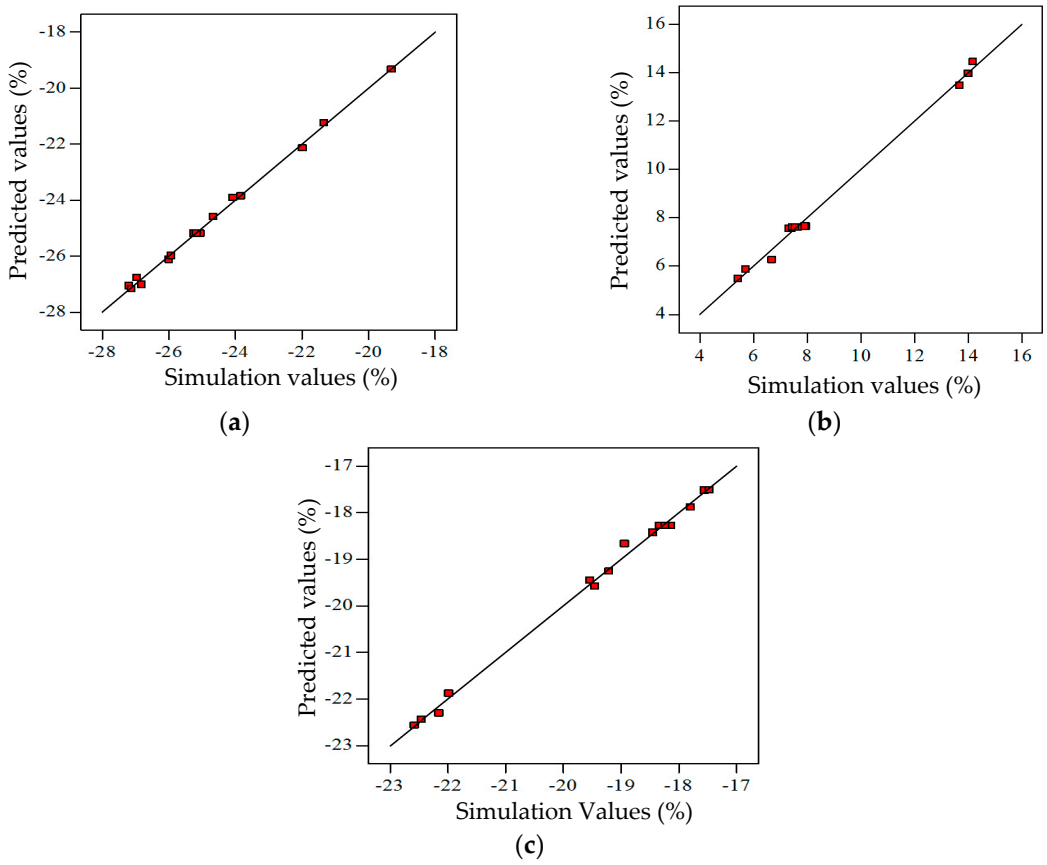

Figure 5. Predicted values versus simulation values for three responses: (**a**) SDR; (**b**) WDO; (**c**) WDI.

3.3.2. Interaction of Important Factors on SDR

From Equation (7), it can be observed that the interaction of Boosting and M clearance, and of Boosting and B clearance, have a significant impact on SDR; and the response surface 3D plots presenting the interactions are drawn based on Equation (7), as shown in Figure 6. From Figure 6a, it can be observed that increasing Boosting and decreasing M clearance led to a decrease in the absolute value of SDR. When the value of Boosting is small, the absolute value of SDR decreases as M clearance decreases, but it decreases very little; just about 1%. When the value of Boosting is large, the decrease of the absolute value of SDR becomes large—about 5%—with the decreasing of M clearance. This means that with the increase of Boosting, the effect of M clearance on SDR becomes more important. As shown

in Figure 6b, the simultaneous increase of Boosting and B clearance reduce the absolute value of SDR. This indicates that the interaction of Boosting and B clearance has a positive effect on SDR. Different from M clearance, the effect of B clearance on SDR is always small with the increase of Boosting.

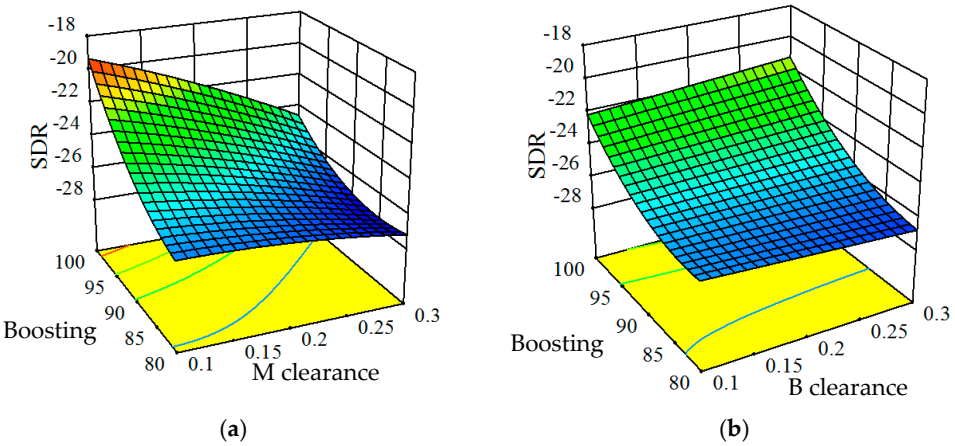

Figure 6. The response surface 3D plots of interaction of important factors on SDR: (**a**) interaction of Boosting and M clearance; (**b**) interaction of Boosting and B clearance.

3.3.3. Interaction of Important Factors on WDO

From Equation (8), it can be found that only the interaction of Boosting and M clearance has a significant influence on WDO. The response surface 3D plot expressing the interaction was drawn according to Equation (8), as shown in Figure 7. It can be seen that the minimum of WDO can be reached in the range of small Boosting and large M clearance. With an increase of Boosting while M clearance remains constant, WDO decreases, but only a little, while WDO decreases greatly with the increasing of M clearance. It can be concluded that M clearance has a more important effect on WDO than Boosting. Increasing M clearance is the most efficient way to decrease WDO. But when M clearance is larger than 0.25 mm, WDO changes little.

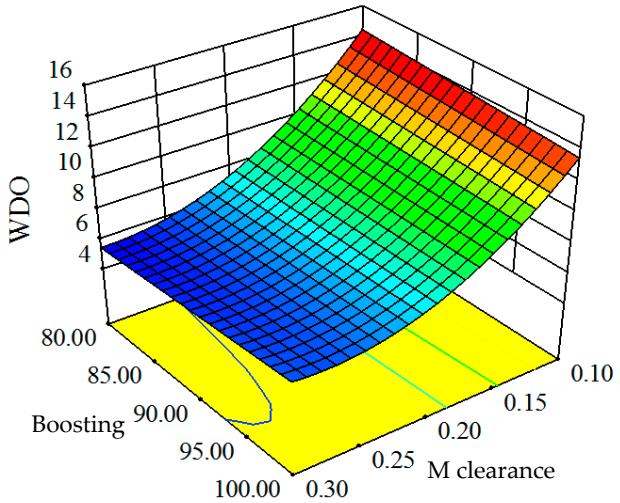

Figure 7. The response surface 3D plots expressing the interaction of Boosting and M clearance on WDO.

3.3.4. Interaction of Important Factors on WDI

From Equation (9), it can be seen that the interaction of M clearance and B clearance and that of B clearance and Boosting have an important impact on WDI; and the response surface 3D plot presenting

the interactions are drawn based on Equation (9), as shown in Figure 8. Figure 8a, it can be seen that the minimum of the absolute value of WDI can be obtained when M clearance reduces from 0.3 mm to 0.1 mm and B clearance increases from 0.1 mm to 0.25 mm. But increasing B clearance continuously will increase the absolute value of WDI. As shown in Figure 8b, with the decrease of Boosting and increase of M clearance, the absolute value of WDI is reduced. But when B clearance increases to near 0.25 mm and Boosting is at a minimum, the minimum of the absolute value of WDI is obtained. Increasing B clearance continuously will make the absolute value of WDI increase.

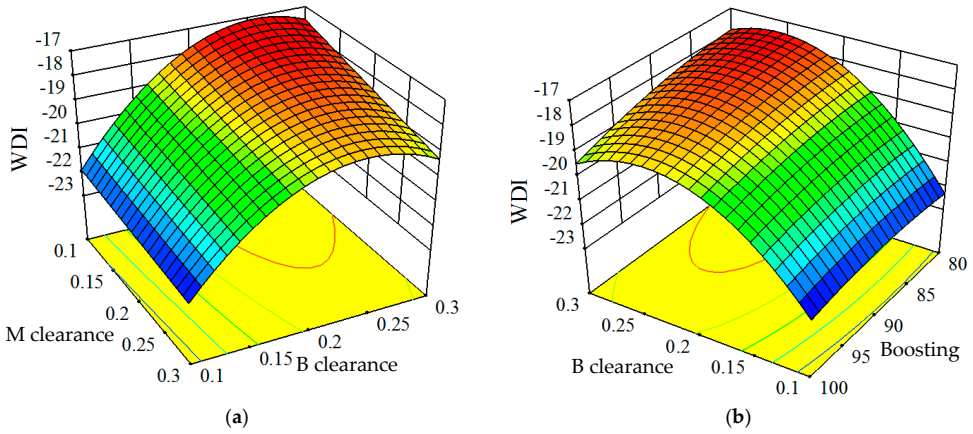

Figure 8. The response surface 3D plots expressing the interaction of factors on WDI: (**a**) interaction of M clearance and B clearance; (**b**) interaction of Boosting and B clearance.

3.4. Multi-Objective Optimization Using NSGA-II

Based on the generated response surface models for SDR, WDO and WDI expressed in Equations (7)–(9), respectively, the multi-objective optimization for cross-sectional deformation of DRRT in RDB was conducted by using NSGA-II. The values of SDR and WDI are negative, so the absolute values of SDR and WDI were adopted to represent their deformation magnitude in order to perform the optimization process conveniently. Minimizing the cross-sectional deformation of DRRT requires the minimization of WDO and the absolute values of SDR and WDI, simultaneously. WDO and WDI have the same impact on the microwave transmission performance of DRRT, so the sum of WDO and absolute value of WDI can be seen as one objective. Eventually, the tri-objective optimization problem was converted into a dual-objective optimization problem. The two objective functions are given below:

$$\text{Objective 1} = |\text{SDR}|, \tag{10}$$

$$\text{Objective 2} = \text{WDO} + |\text{WDI}|, \tag{11}$$

Figure 9 shows the Pareto frontier of dual-objective optimization by using NSGA-II. In the figure, each point located on the Pareto frontier is potentially an optimum solution of the dual-objective optimization problem. The Pareto frontier illustrates an evident conflict between the two objectives. That is to say that the decrease of one objective leads to the increase of another objective in the space of Pareto optimal solutions. The points A and B are the optimal solution of single-objective optimization when one of the two objectives was selected as the objective, respectively. From the set of Pareto optimal solutions in Figure 9, the corresponding values of WDO and WDI in the space of Pareto optimal solutions can be obtained. Figure 10a shows the Pareto frontier of WDO and SDR, from which it can be observed that there is an evident conflict between SDR and WDO. Decreasing the absolute value of SDR from 27.2% to 22.8% does not significantly increase WDO. When the absolute value of SDR decreases from 22.8% to 18.9%, WDO increases sharply. The Pareto frontier of SDR and WDI is shown in Figure 10b and it was found that when the absolute value of SDR decreases from 27.2% to 22.8%, the absolute value of WDI increases almost linearly and this illustrates that there is an evident

conflict between SDR and WDI. But decreasing SDR continually from 22.8% would lead to a decrease in the absolute value of WDI, which indicates that there is no conflict between them in this range.

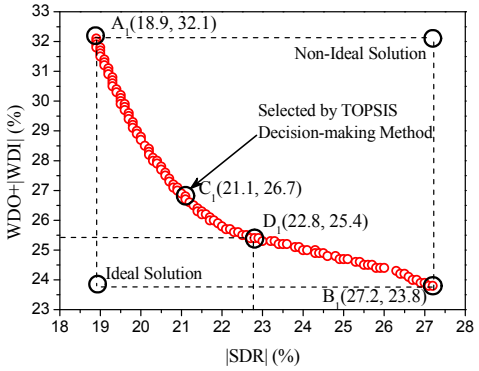

Figure 9. Pareto frontier of dual-objective optimization.

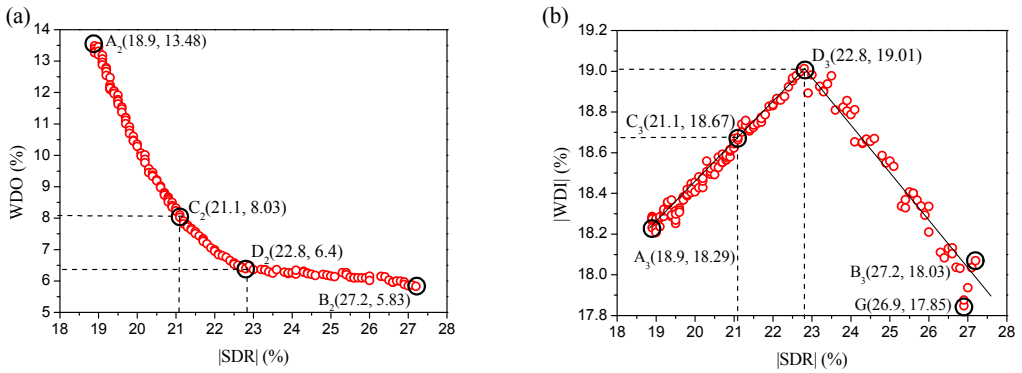

Figure 10. Pareto frontier obtained from dual-optimization: (**a**) the Pareto frontier of WDO and absolute value of SDR; (**b**) the Pareto frontier of the absolute values of WDI and SDR.

For multi-objective optimization problems, all the solutions in the Pareto frontier are non-dominated and can be chosen as the optimal solution. However, only one optimal solution needs to be finally determined in practical operations [15]. There are many methods in the decision-maker process to find the final optimal solution from a Pareto frontier. Before selecting a decision-maker method, the optimal solution set of multi-objective optimization should be non-dimensionalized. The Euclidian method [16] is utilized to conduct the non-dimensionalization procedure according to Equation (12),

$$F_{ij} = \frac{f_{ij}}{\sqrt{\sum_{i=1}^{n} (f_{ij})^2}}, \tag{12}$$

where F_{ij} is the value of ith design point in the Pareto frontier for jth objective and F_{ij}^{n} is the corresponding non-dimensionalization value. After the Pareto optimal solutions were converted into a non-dimensional format, the corresponding Pareto frontier is demonstrated in Figure 11. Then, the decision-maker method, TOPSIS, is used to select the final optimal solution. In this method, the ideal solution and Non-ideal solution need to be determined first. The ideal solution is the one where the optimal solution of single-objective optimization can be obtained for each objective, while the Non-ideal solution is the combination of the worst values of all objectives in the Pareto frontier. The principle of TOPSIS decision-maker method is to find a solution in the Pareto frontier that is closest to the ideal solution and furthest from the Non-ideal solution [17]. For each solution in the Pareto frontier, the distances from the ideal solution D_{i+} and Non-ideal solution D_{i-} are calculated according to Equations (13) and (14), respectively,

$$D_{i+} = \sqrt{\sum_{j=1}^{n} \left(F_{ij} - F_j^{\text{ideal}}\right)^2}, \tag{13}$$

$$D_{i-} = \sqrt{\sum_{j=1}^{n} \left(F_{ij} - F_j^{\text{non-ideal}}\right)^2}, \tag{14}$$

Then, the closeness coefficient Y_i for each solution in the Pareto frontier is derived from Equation (15),

$$Y_i = \frac{D_{i-}}{D_{i+} + D_{i-}}, \tag{15}$$

The solution with the maximum value of closeness coefficient Y_i is selected as the final optimal solution. By using this method, the final solution was determined and defined as point C, as shown in Figure 11. Its corresponding values in Figures 9 and 10 are denoted as points C_1, C_2 and C_3. The final optimal solution of the dual-objective optimization is that SDR, WDO and WDI are −21.1%, 8.03% and −18.67%, respectively. The optimal parameter combination is that M clearance is 0.19 mm, B clearance is 0.26 mm and Boosting of pressure is 100%.

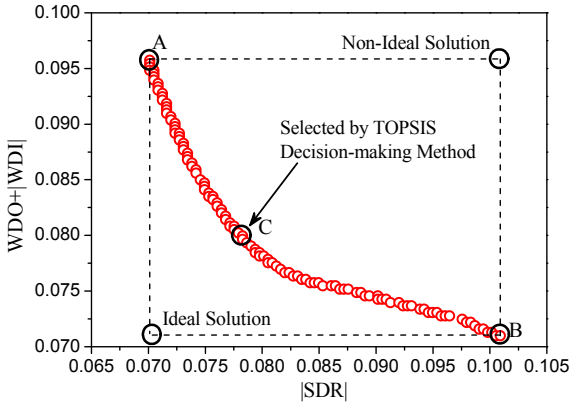

Figure 11. The final optimal non-dimensional solution of dual-objective optimization by using TOPSIS decision-maker method.

After the multi-objective optimization was finished and the optimal results were obtained, a confirmation simulation test was performed using the optimized factors while the other factors were kept constant. The results of the confirmation simulation test are listed in Table 9. It can be seen that the predicted values are highly consistent with the simulation ones for the observed results. This indicates that the proposed method combining RSM and NSGA-II is reliable, and adequate for finding the optimal conditions under which a sound bent DRRT can be obtained in real rotary draw bending. Then, a comparison between the responses before optimization (obtained from the simulation using the parameters shown in Reference [13]) and those after optimization were conducted, as shown in Table 9. It can be seen that the absolute values of SDR and WDI after optimization are 13.17% and 17.97% lower, respectively, than those before optimization, while WDO is just 3.08% higher.

Table 9. Comparison between the responses before optimization and those after optimization.

Responses		|SDR| (%)	WDO (%)	|WDI| (%)
After optimization	Predicted	−21.73	8.06	−18.81
	Simulation	−21.50	8.03	−18.67
Before optimization		24.30	7.79	22.76
Ratio of optimization		−13.17	3.08	−17.97

4. Conclusions

1. By using the orthogonal test design, it was obtained that M clearance, B clearance, and Boosting have an important influence on the cross-sectional deformation of DRRT in RDB. It can also be observed that the variation trend of flange sagging FS is always consistent with that of space deformation between ridges with the changing of factors.
2. The proposed response surface models were used to analyze the relationship of the important parameters to the responses such as space deformation between ridges SDR and width deformation of outer and inner ridge grooves WDO and WDI. Moreover, the interaction of important factors on each response was also better understood.
3. The interaction of responses was revealed and the value range of each response in the space of Pareto optimal solutions was determined by using NSGA-II and the response surface models. It can be observed that there is always an evident conflict between SDR and WDO in the space of Pareto optimal solutions.
4. By using the optimization method of combining RSM and NSGA-II, the absolute values of SDR and WDI were significantly reduced—by 13.17% and 17.97%, respectively—compared with those before optimization, while WDO was increased a little. This confirms that the optimization method is effective for optimizing the processing parameters for reducing cross-sectional deformation of DRRT in RDB.

Acknowledgments: The authors would like to thank the National Natural Science Foundation of China (No. 51375392), Research Fund of the State Key Laboratory of Solidification Processing (NWPU), China (No. 152-ZH-2016) and 111 Project (No. B08040) for the support given to this research.

Author Contributions: Honglie Zhang constructed the response surface models and performed the multi-objective optimization and wrote the paper under the guidance of Yuli liu, and Chunmei Liu assisted in performing experiments and analyzing simulation results.

Conflicts of Interest: The authors declare no conflict of interest.

References

1. Chen, X.Q.; Wu, Q.; Gao, Y.; Lu, M. Multi-objective optimal design of rectangular symmetric double-ridge waveguide. In Proceedings of the 2013 IEEE International Conference on Applied Superconductivity and Electromagnetic Devices, Beijing, China, 25–27 October 2013; pp. 25–27.
2. Li, H.; Hu, X.; Yang, H.; Li, L. Anisotropic and asymmetrical yielding and its distorted evolution: Modeling and applications. *Int. J. Plast.* **2016**, *82*, 127–158. [CrossRef]
3. Zhu, Y.X.; Liu, Y.L.; Yang, H. Sensitivity of springback and section deformation to process parameters in rotary draw bending of thin-walled rectangular H96 brass tube. *Trans. Nonferr. Met. Soc. China* **2012**, *22*, 2233–2240. [CrossRef]
4. Clausen, A.H.; Hopperstad, O.S.; Langseth, M. Sensitivity of model parameters in stretch bending of aluminium extrusions. *Int. J. Mech. Sci.* **2001**, *43*, 427–453. [CrossRef]
5. Yang, H.; Yan, J.; Zhan, M.; Li, H.; Kou, Y.L. 3D numerical study on wrinkling characteristics in NC bending of aluminum alloy thin-walled tubes with large diameters under multi-die constraints. *Comp. Mater. Sci.* **2009**, *45*, 1052–1067.
6. Zhao, G.Y.; Liu, Y.L.; Yang, H. Effect of clearance on wrinkling of thin-walled rectangular tube in rotary draw bending process. *Int. J. Adv. Manuf. Technol.* **2010**, *50*, 85–92. [CrossRef]
7. Lăzărescu, L. FE Simulation and Response Surface Methodology for Optimization of Tube Bending Process. In *The Annals of "Dunărea de Jos" University of Galaţi Fascicle V, Technologies in Mechanical Engineering*; Galati University Press: Galati, Romania, 2010; pp. 93–100.
8. Li, H.; Yang, H.; Xu, J.; Liu, H.; Wang, D.; Li, G. Knowledge-based substep deterministic optimization of large diameter thin-walled Al-alloy tube bending. *Int. J. Adv. Manuf. Technol.* **2013**, *68*, 1989–2004. [CrossRef]
9. Xiao, Y.H.; Liu, Y.L.; Yang, H.; Ren, J.H. Optimization of processing parameters for double-ridged rectangular tube rotary draw bending based on Grey relational analysis. *Int. J. Adv. Manuf. Technol.* **2014**, *70*, 2003–2011. [CrossRef]

10. Yu, S.; Reitz, R.D. Assessment of multiobjective genetic algorithms with different niching strategies and regression methods for engine optimization and design. *J. Eng. Gas Turbines Power* **2010**, *132*, 487–496.
11. Rout, S.K.; Choudhury, B.K.; Sahoo, R.K.; Sarangi, S.K. Multi-objective parametric optimization of Inertance type pulse tube refrigerator using response surface methodology and non-dominated sorting genetic algorithm. *Cryogenics* **2014**, *62*, 71–83. [CrossRef]
12. Padhee, S.; Nayak, N.; Panda, S.K.; Dhal, P.R.; Mahapatra, S.S. Multi-objective parametric optimization of powder mixed electro-discharge machining using response surface methodology and non-dominated sorting genetic algorithm. *Sadhana* **2012**, *37*, 223–240. [CrossRef]
13. Zhang, H.; Liu, Y.; Yang, H. Study on the ridge grooves deformation of double-ridged waveguide tube in rotary draw bending based on analytical and simulative methods. *J. Mater. Process. Technol.* **2017**, *243*, 100–111. [CrossRef]
14. Deb, K.; Pratap, A.; Agarwal, S.; Meyarivan, T. A fast and elitist multiobjective genetic algorithm: NSGA-II. *IEEE. Trans. Evol. Comput.* **2002**, *6*, 182–197. [CrossRef]
15. Shirazi, A.; Aminyavari, M.; Najafi, B.; Rinaldi, F.; Razaghi, M. Thermal-economic-environmental analysis and multi-objective optimization of an internal-reforming solid oxide fuel cell-gas turbine hybrid system. *Int. J. Hydrog. Energy* **2012**, *37*, 19111–19124. [CrossRef]
16. Sayyaadi, H.; Mehrabipour, R. Efficiency enhancement of a gas turbine cycle using an optimized tubular recuperative heat exchanger. *Energy* **2012**, *38*, 362–375. [CrossRef]
17. Yue, Z. A method for group decision-making based on determining weights of decision makers using TOPSIS. *Appl. Math. Model.* **2011**, *35*, 1926–1936. [CrossRef]